

# *Ab initio* study of the uranyl oxide hydrates: a proton transfer mediated by water

S Ostanin<sup>1,2</sup> and P Zeller<sup>1</sup>

<sup>1</sup> Department of Physics and Chemistry, CEA/Saclay, F-91191 Gif sur Yvette, France

<sup>2</sup> Max-Planck-Institut für Mikrostrukturphysik, D-06120 Halle, Germany

E-mail: [sostanin@mpi-halle.mpg.de](mailto:sostanin@mpi-halle.mpg.de)

Received 13 April 2007, in final form 4 May 2007

Published 30 May 2007

Online at [stacks.iop.org/JPhysCM/19/246108](http://stacks.iop.org/JPhysCM/19/246108)

## Abstract

We present a first-principles study of the  $\text{UO}_3 \cdot n(\text{H}_2\text{O})$  uranyl oxide hydrates, namely, schoepite ( $n = 2.25$ ), metaschoepite ( $n = 2$ ) and dehydrated metaschoepite ( $n = 1.75$ ), which appear as the alteration U(VI) products of aqueous corrosion of nuclear fuel. For these compounds, the calculated enthalpy of formation is in good agreement with calorimetry and solubility measurements. We discuss the key electronic state factors behind the phase stability of uranyl oxide hydrates. An unexplored proton-transfer mechanism, which produces the  $\text{H}_3\text{O}^+$  hydronium ions in  $\text{UO}_3 \cdot n\text{H}_2\text{O}$ , has been studied using *ab initio* molecular dynamics simulations at room temperature. For the hydronium ion, a very short lifetime of around 20 fs has been suggested.

(Some figures in this article are in colour only in the electronic version)

## 1. Introduction

In a geological repository of spent nuclear fuel, which is mainly formed of uranium dioxide, any environmental assessment requires a reliable prediction of possible release of U from the nuclear waste that has reacted with groundwater [1].  $\text{UO}_2$  is a thermodynamically unstable compound both in air and water. If the surface oxidation of  $\text{UO}_2$  reaches the composition  $\text{UO}_{2.33}$  it may modify uranium at valence IV to U(VI). When spent fuel is in contact with water, the large quantities of  $\alpha$  and ( $\beta$ ,  $\gamma$ ) radiation emitted from the waste produce the oxidizing radicals  $\text{OH}^*$  and molecular oxidant  $\text{H}_2\text{O}_2$ , which accelerate the U(VI) alteration leading to the radionuclide release.

The hydrated oxides of uranium,  $[\text{UO}_3 \cdot n(\text{H}_2\text{O})]_8$  ( $Z = 4$ ), are naturally generated during an aqueous corrosion of  $\text{UO}_2$ , and several such phases have been reported so far. For these compounds, the crystal structure is extremely complex [2], consisting of  $\text{UO}_2^{2+}$  uranyl ions linked by O and hydroxide ions, which together form a nearly flat polyhedral layer of stoichiometry  $(\text{UO}_2)_4\text{O}(\text{OH})_6$ . For the higher hydrates when  $2.25 > n > 1$ , these layers

are separated by almost planar sheets of the water groups. The largest amount of  $\text{H}_2\text{O}$  was found in schoepite ( $n = 2.25$ ) and metaschoepite ( $n = 2$ ). In air, schoepite slowly transforms to metaschoepite due to a loss of the two (eight)  $\text{H}_2\text{O}$  groups per formula unit (unit cell). The corresponding phase transformation is characterized by a large  $\sim 3\%$  contraction in the direction perpendicular to the U–O layers and relatively moderate  $0.6\%–0.9\%$  contraction in the other dimension [2]. This may suggest that the phase transformation from schoepite to metaschoepite is a more complicated process than the simple removal of  $\text{H}_2\text{O}$ . The structure relationship between metaschoepite and schoepite has been recently discussed in detail by Weller *et al* [3]. However, since the actual positions of hydrogen in these compounds cannot be experimentally detected, some simple arguments were used to establish the H-bonding scheme. In the absence of well-established crystallographic data for the atomic positions of H, it is worthwhile carrying out the *ab initio* optimization of  $\text{UO}_3 \cdot n\text{H}_2\text{O}$  varying the space group and patterns of atomic arrangements. In this paper, from the basis of state of the art *ab initio* calculations, we report on the electronic structures of uranyl oxide hydrates. Since the fundamental nature of aqueous corrosion of  $\text{UO}_2$  is far from being well understood, any theoretical study of products of this reaction (such as schoepite and metaschoepite) becomes very important.

Another area of practical interest in uranyl compounds, in terms of their application to catalysis, is the mechanism of proton transfer from the U–O layers to water layers. Zero-temperature *ab initio* calculations, presented in our work, suggest that some H from the U–O network find their relaxed position, with the lowest energy, in the water layers, forming there the hydronium ion  $\text{H}_3\text{O}^+$ . Proton transfer between Brønsted acids and bases in aqueous solution is a fundamental chemical reaction, the dynamics of which involve different reaction pathways depending on many factors, in particular, the separation between the acid and base molecules. The hopping itself is an ultrafast process accompanied by only modest rearrangements of surrounding shells. For solids, the proton transfer has been extensively studied in zeolites, which are widely used as adsorbents and catalysts. Zero-temperature first-principles calculations of zeolites have reported that the  $\text{H}_3\text{O}^+$  motif appears in some energetically favourable atomic configurations. However, the molecular dynamics (MD) simulations, carried out for zeolites at finite temperature, suggest that the lifetime of hydronium is shorter than 20 fs [4]. For a deeper understanding of the issue of hydronium in  $\text{UO}_3 \cdot n(\text{H}_2\text{O})$ , we use *ab initio* MD simulations described in section 2.

## 2. Method

The study is based on extensive density-functional theory (DFT) calculations [5], in which the effects of relaxation of atomic positions are included. We use the plane-wave pseudopotential code CASTEP [6], where the Perdew–Burke–Ernzerhof (PBE) generalized gradient approximation (GGA-PBE) [7] is used for the exchange and correlation effects. It is generally accepted that CASTEP is one of the most efficient schemes for precise calculation of total energy and forces. This method has also been used to accurately describe the lattice properties of uranium oxides [8]. The electron pseudo-wavefunctions were represented using plane waves, with a cutoff energy of 410 eV, while the electron–ion interactions were described by ultrasoft Vanderbilt pseudopotentials [9] distributed with the code. The distances between the Monkhorst–Pack  $\mathbf{k}$  points in the Brillouin zone were always less than  $0.04 \text{ \AA}^{-1}$ . The relativistic spin–orbit coupling effects upon the electronic structure were omitted. For an insulator, it might not affect the results of optimization. The MATERIALS STUDIO interface software [10] was used for the initiation of calculation and analysis. We

have recently demonstrated that this approach can accurately describe the various properties of uranyl peroxides,  $\text{UO}_4 \cdot n\text{H}_2\text{O}$ , which also appear as important U(VI) products of aqueous corrosion of  $\text{UO}_2$  [11].

For a quantitative description of actinides from first principles, a great deal of care must be taken to ensure that the localized and strongly correlated 5f electrons of U are properly treated. Previous calculations of  $\text{UO}_2$ , made within the local-density approximation (LDA) to DFT or, alternatively, using GGA, found no band gap [8]. This leads to metallic instead of the correct insulating behaviour of  $\text{UO}_2$ . Recently, much work has been conducted to deal with the on-site Coulomb correlations more flexibly. These extensions include the LDA +  $U$  [12] and self-interaction-corrected local spin-density (SIC-LSD) methods [13, 14], and the hybrid Hartree–Fock DFT scheme (HF-DFT) [15]. The use of these techniques [16–18] improved the calculated ground state of  $\text{UO}_2$  to yield an insulating antiferromagnet well established from the experiment. For uranyl peroxides, a reasonably wide insulating gap has been obtained with the use of GGA [11]. Thus, there is no convincing evidence that the uranyl oxide hydrates must be treated using some advanced DFT model beyond LDA/GGA. In this study, we restrict ourselves to the GGA, which provides an appropriate starting point.

We also look in detail at a possible proton transfer between the U–O and water layers of  $\text{UO}_3 \cdot n(\text{H}_2\text{O})$ . It is known from the literature that the  $\text{H}_3\text{O}$  motif [19] can appear in some low-energy atomic configurations of the water-containing materials. Here we use the *ab initio* MD within CASTEP. The time step used in our MD simulations was 1 fs. To obtain adequate statistics for thermodynamic equilibrium, we ran the simulations for a time of 3 ps. The temperature was 300 K. Simulations were started from the well-relaxed atomic arrangements and equilibrium unit cell parameters.  $\Gamma$ -point Brillouin zone sampling was used.

### 3. The crystal structure

The structure of schoepite is orthorhombic [2] with space group symmetry  $P2(1)ca$  and a measured unit cell volume of  $3551 \pm 2 \text{ \AA}^3$  ( $Z = 4$ ). This volume corresponds to the lattice parameters  $a = 14.337 \text{ \AA}$ ,  $b = 16.813 \text{ \AA}$  and  $c = 14.731 \text{ \AA}$ . Each formula unit,  $Z$ , contains 8 U atoms, 24 O and 18  $\text{H}_2\text{O}$  groups. The  $\text{H}_2\text{O}$  groups form planar sheets stacking along the  $c$ -axis.

The unit cell of schoepite contains two U–O layers and two water layers. Assuming that the U–O layers weakly interact to each other through the separating water layer, we have made a simplification using half of the unit cell  $a \times b \times \frac{c}{2}$ , with space group symmetry  $P2(1)$ . Thus, all our *ab initio* calculations were made using this model unit cell while the equilibrium volume and  $c$ -axis value were then doubled to compare with the experimental data. In figure 1, we plot half of the unit cell  $a \times b \times \frac{c}{2}$  after the volume optimization and relaxation of atomic positions. For schoepite, we obtain the equilibrium volume of  $3627.1 \text{ \AA}^3$ , which is  $\sim 2.1\%$  larger than the experimentally determined value. All calculated lattice parameters  $a = 14.387 \text{ \AA}$ ,  $b = 16.893 \text{ \AA}$  and  $c = 14.924 \text{ \AA}$  are in good agreement with the experimental data given above. Since the calculated total energy of schoepite weakly depends on the orientation of the water molecules, it may justify *a posteriori* the structural simplification made in our work when half of the schoepite unit cell was used.

Each uranium of schoepite is strongly bonded to two O, resulting in a linear  $\text{UO}_2^{2+}$  uranyl ion. Its U–O bond length varies between 1.814 and 1.88  $\text{ \AA}$ , while the corresponding calculated Mulliken population changes from 0.79 to 0.72. The spatial orientation of  $\text{UO}_2^{2+}$  can be considered as dual, with an average  $15^\circ$  deviation angle from the [001] direction. In an equatorial plane perpendicular to the O–U–O uranyl group, uranium is bonded to four or

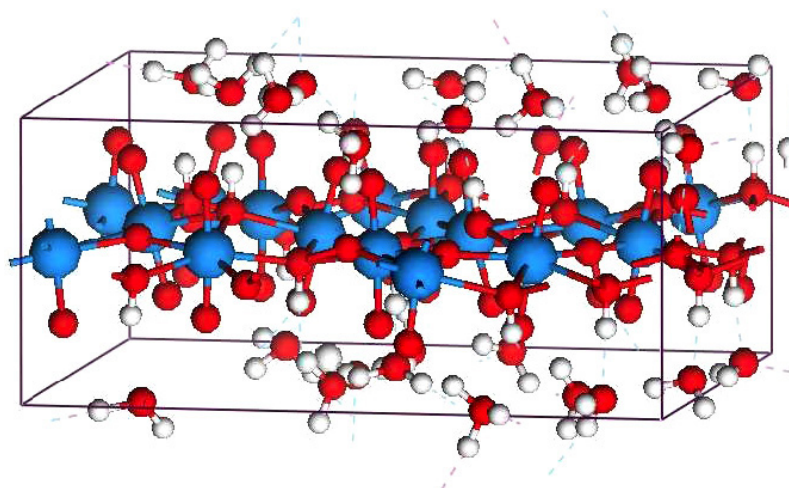


**Figure 1.** The relaxed schoepite structure plotted as half of unit cell  $a \times b \times \frac{c}{2}$  ( $Z = 2$ ). The larger spheres represent uranium and the smaller dark and white spheres show oxygen and hydrogen respectively.

five O, with the bond variation of  $2.14 \text{ \AA} < d < 2.65 \text{ \AA}$ . These O atoms form a nearly flat polyhedral layer of stoichiometry  $(\text{UO}_2)_4\text{O}(\text{OH})_6$ , shown in figure 2. Since the  $\text{UO}_2^{2+}$  ions may have a dual orientation, the U–O bonds of the  $(\text{UO}_2)_4\text{O}(\text{OH})_6$  layer tend to form a zig-zag as seen in figure 1. As a result, all O in this network alternatively move up and down on a 1:1 basis from the layer plane forming the vertices of pentagonal bipyramids. For the U–O network, the shortest U–O bond of  $2.14 \text{ \AA}$  has the Mulliken population value of 0.42 whereas the most distant O from uranium, which appears as its fifth in-plane nearest neighbour, has the relatively low bond population of 0.11. It has already been shown that the use of GGA for the uranyl compounds tends to overestimate both the unit cell volume and interatomic bond lengths [11] compared to the experiment. For schoepite, the computed bond lengths are always larger than the corresponding measured values [3], but they do not affect the key conclusions on the optimized crystal structure and band structure.

In the U–O layers of schoepite before relaxation, all oxygen atoms, with the two exceptions per each Z, form hydroxyl groups. This is based on the literature data, obtained with the use of a simple model known as the bond-valence sums [20]. The hydroxide bonds are oriented roughly perpendicular to the U–O sheets. The number of hydroxide groups in schoepite is equal to the number of  $\text{H}_2\text{O}$  between the U–O layers. Therefore, one can assume that each hydroxide is weakly bonded to the different  $\text{H}_2\text{O}$  group. After relaxation, the result of which is shown in figure 3, we find that the three H atoms break their hydroxide group and move toward the water group. Hence, the number of HO reduces from 12 to 9 for each formula unit. In the water layer, an appearance of extra H results in the three  $\text{H}_3\text{O}^+$  hydronium ions, reducing the number of  $\text{H}_2\text{O}$  from 12 to 9 per formula unit, Z. For the  $\text{H}_3\text{O}^+$  ions, we have calculated the bond lengths and angles and the bond population. The two shorter ‘waterlike’ H–O separations vary between  $1.02$  and  $1.04 \text{ \AA}$ , while the corresponding bond population changes from 0.56 to 0.51. The third and most distant H from oxygen in  $\text{H}_3\text{O}^+$  has the bond length of  $\sim 1.1 \text{ \AA}$ , with the population value of 0.42. The average bond angles of  $\text{H}_3\text{O}^+$  are  $105.8^\circ \pm 1^\circ$ ,  $107.8^\circ \pm 1^\circ$  and  $112^\circ \pm 3^\circ$ . In section 6, we discuss the lifetime issue for the hydronium ion.

The name metaschoepite was chosen because it is a reversible product of partial dehydration of schoepite. In terms of chemical composition,  $(\text{UO}_3 \cdot n\text{H}_2\text{O})_8$ , the only difference

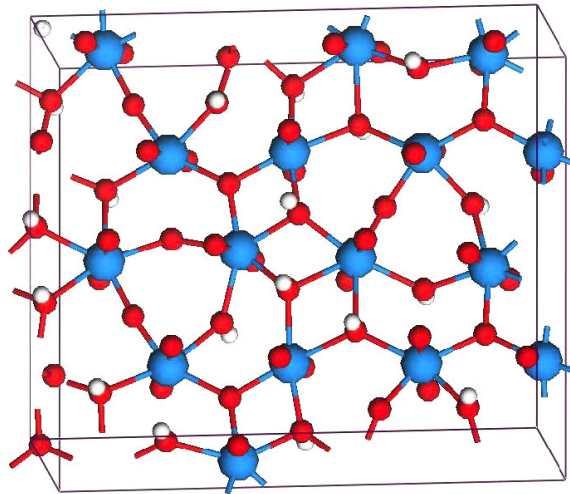


**Figure 2.** The unit cell fragment of the  $(\text{UO}_2)_4\text{O}(\text{OH})_6$  layer of schoepite after relaxation.

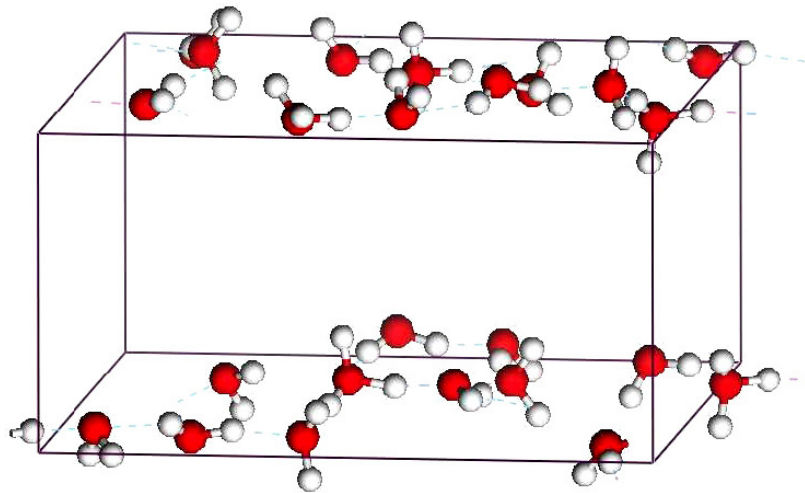


**Figure 3.** The relaxed positions of the  $\text{H}_2\text{O}$  groups and  $\text{H}_3\text{O}^+$  ions in the water layers of schoepite. The dark and white spheres indicate O and H.  $(\text{UO}_2)_4\text{O}(\text{OH})_6$  layer between the two water layers is not shown.

between schoepite ( $n = 2.25$ ) and metaschoepite ( $n = 2$ ) is the two water molecules per formula unit,  $Z$ . However, the actual arrangements of atoms in metaschoepite, compared to those of schoepite, show that the phase transformation is not just a removal of  $\text{H}_2\text{O}$  from the ‘water’ layers. Experiments reveal [2] that metaschoepite has orthorhombic space group  $Pbna$ , with lattice parameters 13.99, 16.72, 14.73 Å and volume  $V = 3445.54 \text{ \AA}^3$ . For a synthetic single crystal of metaschoepite measured at 150 K, Weller *et al* [3] have reported the volume of  $3429.97 \text{ \AA}^3$ . We have optimized the atomic positions and volume of metaschoepite and dehydrated metaschoepite ( $n = 1.75$ ), using half of the unit cell as before for the schoepite case. Regarding the equilibrium volume, there is gradually worsening agreement from schoepite to dehydrated metaschoepite between the theory and experiment. For metaschoepite, the

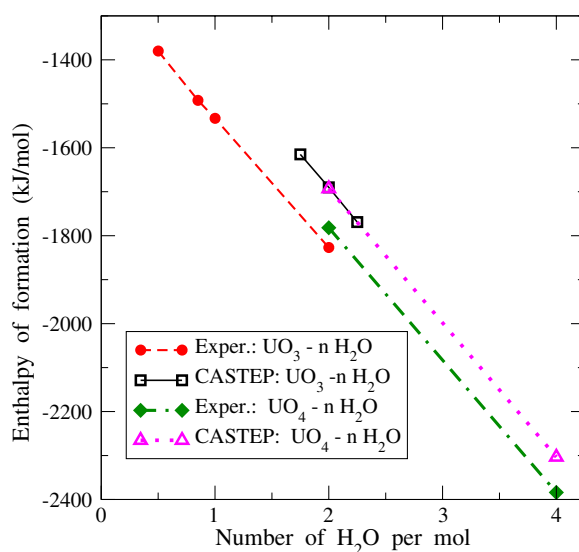


**Figure 4.** Enthalpy of formation  $\Delta H$  for the uranyl oxide hydrates and uranyl peroxides, calculated from first principles and plotted in comparison with the experimental data from [21].

theoretical volume is about 6% larger than the measured value. We believe that the deviation might be reduced when a complete unit cell is optimized. Weller *et al* [3] have reported that small differences between schoepite and metaschoepite exist in both the directions of uranyl ion and orientation of pentagonal bipyramids within the U–O network. The explanation is rather simple. When  $n \leq 2$  there is a deficit of H<sub>2</sub>O to form a link with the nearest HO ion on a 1:1 basis. Therefore, some ions of the U–O network get more freedom. For schoepite, the initial ratio between the number of H<sub>3</sub>O and H<sub>2</sub>O is 1:3, obtained at  $T = 0$  K after the static optimization. During dehydration, this ratio gradually decreases to 1:4 in metaschoepite and, finally, to 1:7 in dehydrated metaschoepite.

#### 4. Enthalpy of formation

For schoepite, the enthalpy of formation  $\Delta H$  from the elements



is  $-1769$  kJ mol<sup>-1</sup>, calculated at  $T = 0$  K for the equilibrium volume with the use of CASTEP. This means that schoepite might be an energetically favourable composition relative to metal U and H<sub>2</sub> and O<sub>2</sub> in their gas states. For metaschoepite and dehydrated metaschoepite ( $n = 1.75$ ), the calculations of  $\Delta H$  yield  $-1690$  kJ mol<sup>-1</sup> and  $-1615$  kJ mol<sup>-1</sup>, respectively. In figure 4, we plot  $\Delta H$  as a function of the number  $n$  of water molecules in  $\text{UO}_3 \cdot n(\text{H}_2\text{O})$  together with the calorimetry data [21]. The deviation between the measured and calculated  $\Delta H$  values is within 10%–12%. Each set of  $\Delta H$  forms a nearly linear curve, with the same negative slope  $\Delta H/\Delta n \approx -300$  kJ (mol  $\times$  n)<sup>-1</sup>, the value of which is in excellent agreement with the experimental  $\Delta H = -285.8$  kJ mol<sup>-1</sup> for water in its liquid state.

In figure 4, we also plot the enthalpy of formation for uranyl peroxides [11]. For the  $\text{UO}_4 \cdot n\text{H}_2\text{O}$  compounds, CASTEP yields a better agreement with calorimetry, underestimating the magnitude of  $\Delta H$  by  $\sim 5\%$ . The systematic shift, seen in the calculated  $\Delta H$  for the two families of compounds, can partially come from the reference energies. It has been found

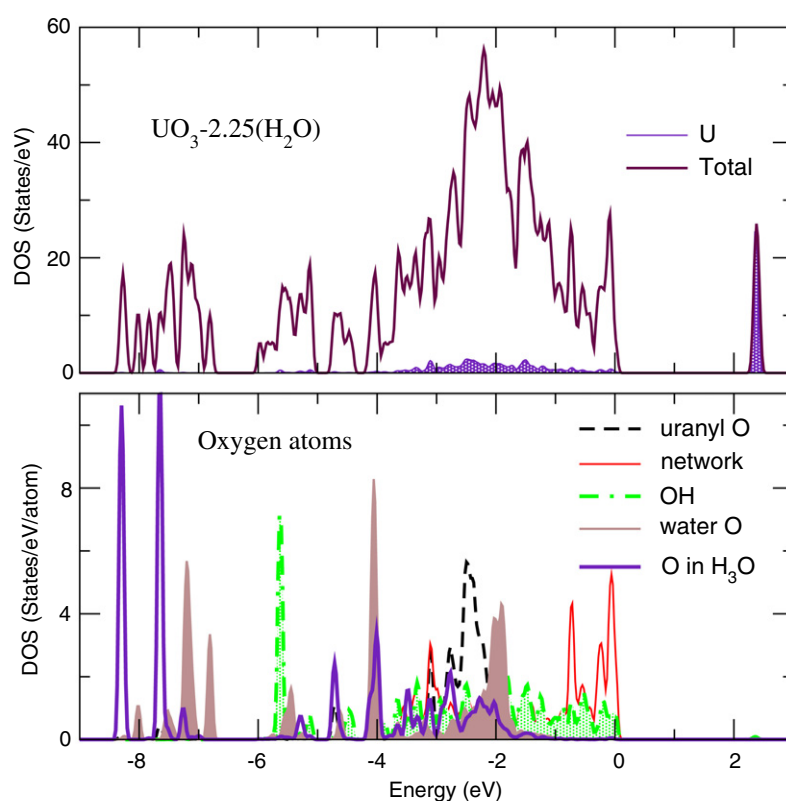


**Figure 5.** The total and U-resolved DOS of schoepite are plotted in the upper panel. The top of the valence band is taken as zero energy. The O-projected DOSs are plotted in the lower panel for the five types of oxygen in schoepite.

that the use of GGA leads to a discrepancy of  $56 \text{ kJ mol}^{-1}$  in the dissociation energy of the oxygen molecule with respect to experiment. Apparently, the two sets of  $\Delta H$ , calculated for the different uranyl compounds and plotted in figure 4, are in a single straight line, whereas the corresponding experimental data form the two clearly distinguished curves. Regarding the CASTEP data plotted in figure 4, we believe that their single-line behaviour is the result of 0 K calculations. For the room-temperature simulations, the enthalpy contributions from atomic vibrations of each compound must split the single  $\Delta H$  line into the two curves, improving the overall agreement with experiment.

## 5. The electronic states

The total and Mulliken site- and state-projected density of states (DOS) of schoepite are derived from the energy bands after the cell optimization and relaxation of atomic coordinates. In the case of an insulator, the separation between the occupied and empty energy bands can be associated with the experimental band gap. The total DOS, which is plotted in the upper panel of figure 5, shows a pronounced insulating band gap of 2.3 eV. Since, so far, the corresponding measurements for schoepite are not available, it is possible to speculate that the fundamental gap value may be underestimated, when the GGA approximation to DFT is used. Comparing the DOS of  $\text{UO}_2$ , known from the literature [17], and the DOS of schoepite we see a spectacular

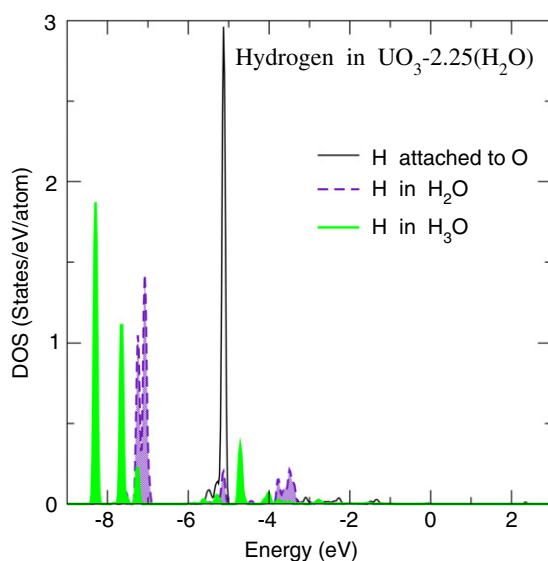


**Figure 6.** The H-resolved DOS are plotted for each type of H in schoepite.

change of the occupied electronic states in schoepite occurring due to aqueous corrosion. In pure  $\text{UO}_2$ , both the upper multipeak valence band and conduction band are formed mainly by the 5f states of U. In the upper panel of figure 5, we plot the U-projected DOS of schoepite with the top of the valence band corresponding to  $E = 0$  eV. For schoepite, the major DOS features can be summarized as follows. The lower conduction band is entirely formed by the f states of U, whereas the upper valence band is mainly composed of the five types of O atom.

In the lower panel of figure 5, we plot the O-resolved 2p DOS for each type of O atom of schoepite. The occupied 2p O band extends from 0 to  $-8.5$  eV binding energy, with a pseudogap of 1 eV between  $-5.8$  and  $-6.8$  eV. The first two O DOS peaks just below the top of the valence band between  $-1$  eV and  $E = 0$ , come from the network-O states. Besides, the O atoms of hydroxide group also contribute to the DOS in this region. The occupied O DOS peaks seen at  $E \sim -2$  and  $-2.5$  eV are associated with the  $\text{H}_2\text{O}$ -group and oxygen in  $\text{UO}_2^{2+}$ , respectively. The numerous O atoms of the uranyl ions yield the main DOS feature at around  $-2.5$  eV. All other significant O p DOS peaks below  $E < -4$  eV are very narrow in their energy position, which reflects a strongly localized molecular character for these electronic states. The O atoms of the water groups contribute to the DOS at  $-4$  eV and also at around  $-7$  eV. The O atoms of the hydroxide groups yield the DOS peak at  $E \sim -5.5$  eV. However, the most pronounced O DOS peaks, seen in the lower panel of figure 5 far below the Fermi level at  $\sim -8$  eV, come from the  $\text{H}_3\text{O}$  ion.

The s states of hydrogen contribute to the DOS below  $E < -5$  eV. It is helpful to classify the H atoms in  $\text{UO}_3 \cdot n(\text{H}_2\text{O})$ . There are the three types of H: (i) the H atom of the HO ion adjacent to U, (ii) hydrogen in  $\text{H}_2\text{O}$  and (iii) hydrogen which breaks its HO and appears as the most distant proton in  $\text{H}_3\text{O}$ . In figure 6, we plot the DOS curves, calculated for each type of hydrogen. The first pronounced H DOS peak seen at  $-5$  eV, comes from hydrogen of the hydroxide group. Then, in the lower energy region the H atoms of the water and  $\text{H}_3\text{O}$  groups contribute to the DOS around  $E \approx -7$  and  $-8$  eV. Thus, the electronic states, associated with the  $\text{H}_2\text{O}$  and  $\text{H}_3\text{O}$  groups, dominate in the energy region  $-8.5$  eV  $< E < -6.8$  eV, i.e. far below the Fermi level.

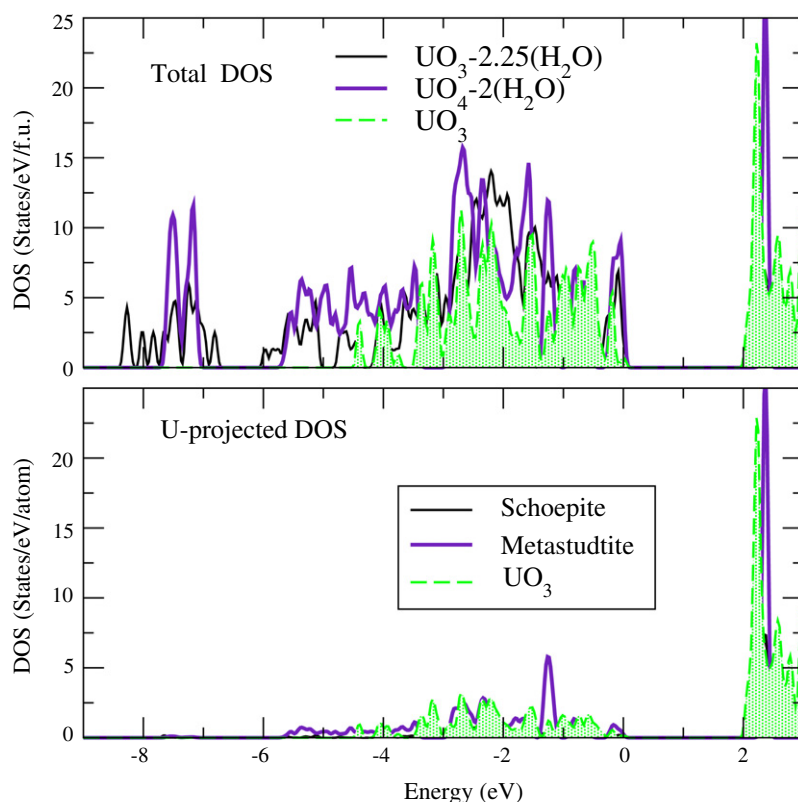


**Figure 7.** The total DOS of schoepite is plotted in the top panel in comparison with those of metastudtite and  $\text{UO}_3$ . In the lower panel, the corresponding U-resolved DOS is shown for each compound.

Regarding the conduction band of schoepite, the first significant DOS feature, which appears at 2.3 eV, comes from the U f states. In fact, the DOS of schoepite is similar to those of uranyl peroxides [11] and thermally stable ceramics, such as stabilized zirconias (see, for instance [22, 23]), where the top of the valence band is also formed by the 2p O states while the unoccupied cation states dominate the bottom of the conduction band. These findings help to understand the similarities between the ground states of different but stable products of oxidation.

All uranyl-containing compounds become stable depending on the underlying electronic structure when the U(VI) complex is formed. Figure 7 shows the DOS of schoepite compared with those of metastudtite and  $\text{UO}_3$ . Since  $\text{UO}_3$  can be considered as the final product of oxidation of  $\text{UO}_2$ , it is possible to directly compare its DOS with those of uranyl peroxides and uranyl oxide hydrates. This may reveal the key electronic states factors behind the phase stability of the U(VI) compounds. We have calculated the  $\delta$ -phase of  $\text{UO}_3$ , with space group symmetry  $Pm\bar{3}m$ . The band gap of  $\text{UO}_3$  is 2 eV. In the case of uranyl compounds, our calculations yield a wider band gap of 2.3 eV when the same DFT approximations are used. The occupied DOS of uranyl compounds are similar to each other and to that of  $\text{UO}_3$ . In particular, the upper valence band is largely formed by the 2p O states. For metastudtite, the top of the valence band is formed by the peroxide O atoms whereas the O network atoms form the top of the occupied DOS in  $\text{UO}_3 \cdot n(\text{H}_2\text{O})$ . Below the Fermi level, the 2p O states form a wide energy

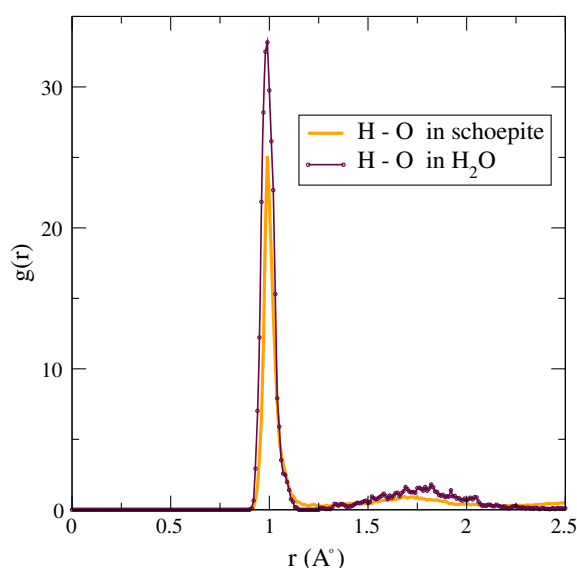


**Figure 8.** Radial distribution functions  $g_{\text{H-O}}(r)$  for schoepite and water.

band with the U-projected electronic states. In the case of uranyl compounds, this energy band extends down to  $E = -6$  eV, that is about 2 eV larger than the valence band of  $\text{UO}_3$ . One of the interesting points to come out of our calculation is that the p states of those O atoms, which are strongly bonded to U, play a crucial role on the stabilization process of the uranyl compounds. In  $\text{UO}_3 \cdot n(\text{H}_2\text{O})$ , the network O atoms play such a role. The spatial orientation of the H–O bonds and their amount in the HO,  $\text{H}_2\text{O}$  and  $\text{H}_3\text{O}$  groups is also very important when the precise energetics is calculated.

## 6. Molecular dynamics simulations

Zero-temperature first-principles calculations reveal that proton transfer, which can take place in the uranyl oxide hydrates, yields an association of  $\text{H}_3\text{O}$ . We apply the *ab initio* MD option of CASTEP and run the simulations for 0.3 ps at 300 K, starting from the relaxed model cell of schoepite. At room temperature, our MD simulations show that the H–O bond lengths and angles in the water layers are quickly changed. Besides, both the  $\text{H}_3\text{O}$  and  $\text{H}_2\text{O}$  groups additionally obtain rotational degrees of freedom. This is the case for all simulations, regardless of the starting conditions and concentration of  $\text{H}_2\text{O}$ . In one case, such an exotic ion as the Zundel cation  $\text{H}_5\text{O}_2$  has been detected. For the hydronium ion, we see that one of its H, but not necessarily that which initially was the most distant, moves away from oxygen so that the separation between them exceeds 1.12 Å within 17–20 fs. Therefore, a time of 20 fs can be considered as the hydronium lifetime, assuming that the H–O bond length larger than 1.12 Å is a breaking distance. Thus, the lifetime value of  $\text{H}_3\text{O}$  in  $\text{UO}_3 \cdot n(\text{H}_2\text{O})$  may be similar to that of zeolites. In  $\text{UO}_3 \cdot n(\text{H}_2\text{O})$ , however, the proton, which breaks the hydronium ion, never goes too far from its own water molecule. It can come back closer to O and when their separation becomes less than 1.12 Å the recombination of  $\text{H}_3\text{O}$  formally takes place. As has been detected from our MD simulation, all bond lengths of  $\text{H}_3\text{O}$  vary between 0.96 and 1.26 Å, and sometimes such a change can happen for the time period of <0.1 ps.

To reveal the similarities and differences between water and  $\text{H}_3\text{O}$ , we calculate the partial radial distribution function (RDF). The RDF,  $g_{\alpha,\beta}(r)$ , is defined so that sitting on an  $\alpha$ -atom the

probability of finding the  $\beta$ -atom in the spherical shell  $(r, r + dr)$  is  $4\pi r^2 n_\beta g_{\alpha,\beta}(r) dr$ , where  $n_\beta$  is the number density of the  $\beta$  species. When  $\alpha = \text{H}$  and  $\beta = \text{O}$  the first maximum of  $g(r)$ , calculated over the long-time interval, corresponds to the equilibrium H–O distance, as is shown in figure 8. It is interesting to compare the RDF of schoepite with that of water, which is also plotted in figure 8.  $\text{H}_2\text{O}$  was simulated using the *ab initio* MD and a large supercell, within the GGA, at  $T = 300$  K and zero pressure. In figure 8 the first maximum of  $g_{\text{H-O}}$  is seen at  $\sim 1$  Å for the calculated RDFs. In the case of water, (i) the main RDF peak is significantly large and slightly wider than that of schoepite, and (ii) there are no bonds between 1.15 and 1.3 Å because the second RDF peak, seen at  $\sim 1.8$  Å, corresponds to the next-nearest neighbour. For schoepite, the appearance of  $g_{\text{H-O}} > 0$  at around 1.2 Å is a clear evidence that the H atoms pose a challenge for the hydronium recombination. Fortunately, we are able to see that by inspecting many snapshots.

## 7. Conclusions

In summary, from the *ab initio* basis of our work we have studied the crystal structure and electronic states of the uranyl oxide hydrates, known as schoepite and metaschoepite, which are the stable phases of wet oxidation of  $\text{UO}_2$ . For these compounds, the calculated enthalpy of formation is in good agreement with experiment while the deviation is within 12%. Uranyl oxide hydrates possess a strong anisotropy, resulting in the puckered U–O network and ‘waterlike’ layers alternating in the [001] direction. The U–O network and uranyl ions, oriented perpendicularly each other, form the highest oxidation state U(VI). Applying the generalized gradient approximation to the DFT exchange–correlation potential, the insulating gap value of 2.3 eV has been obtained. For the electronic states of uranyl oxide hydrates, the upper valence band is always composed by the U–O network’s O 2p states, while the lower conduction band is composed by the U 5f states. We have explored the possible dissociation of  $\text{H}_3\text{O}$  in  $\text{UO}_3 \cdot n\text{H}_2\text{O}$  followed by its reassociation, using *ab initio* molecular dynamics simulations at room temperature. For the hydronium ion, the lifetime is found to be very short, around 20 fs, in excellent agreement with earlier studies on zeolites. We believe that infrared (IR) spectroscopy might be a useful tool to provide evidence favouring our findings on  $\text{H}_3\text{O}$ .

## Acknowledgment

This work was supported by the PRECCI project (CEA and EDF, France).

## References

- [1] Corbel C, Sattonnay G, Guilbert S, Garrido F, Barthe M F and Jegou C 2006 *J. Nucl. Mater.* **348** 1
- [2] Finch R J, Cooper M A, Hawthorne F C and Ewing R C 1996 *Can. Mineral.* **34** 1071  
Finch R J, Hawthorne F C and Ewing R C 1998 *Can. Mineral.* **36** 831
- [3] Weller M T, Light M E and Gelbrich T 2000 *Acta Crystallogr. B* **56** 577
- [4] Li H, Mahanti S D and Pinnavaia T J 2005 *J. Phys. Chem. B* **109** 21908
- [5] Martin R M 2004 *Electronic Structure Basic Theory and Practical Methods* (Cambridge: Cambridge University Press)
- [6] Segall M D, Lindan P J D, Probert M J, Pickard C J, Hasnip P J, Clark S J and Payne M C 2002 *J. Phys.: Condens. Matter* **14** 2717
- [7] Perdew J P, Burke K and Ernzerhof M 1996 *Phys. Rev. Lett.* **77** 3865
- [8] Pickard C J, Winkler B, Chen R K, Payne M C, Lee M H, Lin J S, White J A, Milman V and Vanderbilt D 2000 *Phys. Rev. Lett.* **85** 5122
- [9] Vanderbilt D 1990 *Phys. Rev. B* **41** 7892

- [10] <http://www.accelrys.com>
- [11] Ostanin S and Zeller P 2007 *Phys. Rev. B* **75** 073101
- [12] Anisimov V I, Aryasetiawan F and Lichtenstein A I 1997 *J. Phys.: Condens. Matter* **9** 767
- [13] Perdew J P and Zunger A 1981 *Phys. Rev. B* **23** 5048
- [14] Petit L, Svane A, Szotek Z and Temmerman W M 2003 *Science* **301** 498
- [15] Kudin K N, Scuseria G E and Martin R L 2002 *Phys. Rev. Lett.* **89** 266402
- [16] Dudarev S L, Castell M R, Botton G A, Savrasov S Y, Muggelberg C, Briggs G A D, Sutton A P and Goddard D T 2000 *Micron* **31** 363
- [17] Prodan I D, Scuseria G E and Martin R L 2006 *Phys. Rev. B* **73** 045104
- [18] Laskowski R, Madsen G K H, Blaha P and Schwarz K 2004 *Phys. Rev. B* **69** 140408(R)
- [19] Mohammed O F, Pines D, Dreyer J, Pines E and Nibbering E T J 2005 *Science* **310** 83
- [20] Brown I D and Altermatt D 1985 *Acta Crystallogr. B* **41** 244
- [21] Katz J J, Seaborg G T and Morss L R (ed) 1986 *The Chemistry of the Actinide Elements* vol 2 (New York: Chapman and Hall)
- [22] Ostanin S, Craven A J, McComb D W, Vlachos D, Alavi A, Paxton A T and Finnis M W 2002 *Phys. Rev. B* **65** 224109
- [23] Ostanin S, Ernst A, Sandratskii L, Bruno P, Däne M, Hughes I D, Staunton J B, Hergert W, Mertig I and Kudrnovský J 2007 *Phys. Rev. Lett.* **98** 016101